Glycoconjugate Journal 18, 309–320, 2001
© 2002 Kluwer Academic Publishers. Manufactured in The Netherlands.

Profiling with structural elucidation of the neutral and anionic O-linked oligosaccharides in the egg jelly coat of *Xenopus laevis* by Fourier transform mass spectrometry

Ken Tseng[1], Yongming Xie[1], Juliette Seeley[1], Jerry L. Hedrick[2] and Carlito B. Lebrilla[1]*

[1] *Department of Chemistry, and* [2] *Section of Molecular and Cellular Biology, University of California, Davis, Davis, CA 95616*

A strategic method with high speed and sensitivity is outlined for the analysis of mucin-type oligosaccharide from the jelly coat of *Xenopus laevis*. The method relies primarily on mass spectrometric techniques, in this case matrix-assisted laser desorption/ionization Fourier-transform mass spectrometry (MALDI-FTMS) and collision-induced dissociation (CID). Separation with isolation of the oligosaccharides was streamlined to couple well with mass spectrometry allowing the rapid determination of all detectable components from both neutral and anionic species. Partial structures of anionic components, composed primarily of sulfate esters, were obtained with CID. For neutral species, a method that allowed the complete structural determination using mass spectrometry was used. The method builds on the structure of small number of known compounds to determine unknown structures from the same biological source. In this example, a small number of oligosaccharides, elucidated previously by NMR, were used to develop a set of substructural motifs that were characterized by CID. The presence of the motifs in the CID spectra were then used to determine the structures of unknown compounds that were in abundances too small for NMR analysis.

Keywords: Fourier transform mass spectrometry, MALDI, collision-induced dissociation, catalog-library approach, *Xenopus laevis*

Introduction

Oligosaccharide moieties of glycoproteins play important roles in cellular recognition [1]. The large variation and complexity of oligosaccharide structures allows diverse biological information to be encoded within them. However, the major barrier towards understanding the biochemistry of oligosaccharides is the lack of rapid methods for structure determination. Consequently, it is difficult to establish the connection between the structure of an oligosaccharide and its biological function. Oligosaccharides released from biological sources produce structurally heterogeneous mixtures. This often means that tedious purification and isolation steps are required. The small amount of sample available from biological sources is a further limitation.

Xenopus laevis, the South African frog, has been studied extensively to understand the fertilization process [2–6]. Oligosaccharides from the egg jelly glycoproteins are known to be essential in fertilization events. Their function may include protection of eggs against pathogens, initiation of sperm capacitation or the acrosome reaction, species-specific interaction of gametes, and prevention of polyspermy [2,6]. It has also been postulated that a role oligosaccharides play in fertilization events may be to provide definite structural recognition sites [7]. Since many egg jelly glycoprotein oligosaccharides are anionic, they may also provide a microenvironment around the egg that is required for the occurrence of a successful fertilization [8,9].

Under electron microscopy, the glycoproteins in mucins appear to have brush-like structures [10]. The O-linked oligosaccharides are highly heterogeneous in structure. In the present study, we find nearly 30 neutral and over 47 anionic O-linked oligosaccharide components in the egg jelly glycoproteins. A challenge in analyzing mixtures of this complexity is that complete separation of the individual oligosaccharides by chromatography or electrophoresis is a prerequisite to many structural elucidation methods. Currently, only multidimensional NMR can achieve complete structural elucidation of oligosaccharides [11,12]. However, the sample

*To whom correspondence should be addressed.

amount required often exceeds that which is available. Enzymatic methods can be used but the number of specific exoglycosidases and endoglycosidases is limited [13,14]. Other methods, such as chemical degradation, are available but they often require considerable time and effort and are not sufficiently specific. Furthermore, they often lack the sensitivity required for the direct analysis of biological samples.

Mass spectrometry has become an important tool in the analysis of oligosaccharides [15–18]. Matrix-assisted laser desorption/ionization coupled with Fourier-transform mass spectrometry (MALDI-FTMS) offers high resolving power and high sensitivity and makes it especially suited for analyzing mixtures of oligosaccharides [19,20]. The time-consuming steps of isolation and purification of individual oligosaccharides can be minimized, because mixtures can be elucidated readily by FTMS. Isomers pose some difficulty, but we find that even rudimentary separation with, for example, HPLC is often sufficient for analysis by FTMS.

A rapid and simple method for the analysis of O-linked oligosaccharide libraries is proposed that employs only rudimentary separation and mass spectrometry primarily as the tool for analysis. No derivatization is needed. The specific separation of neutral and anionic oligosaccharides by anion-exchange chromatography is avoided. With mass spectrometry, neutral and anionic oligosaccharides are analyzed simply in positive and negative mode, respectively. Preparation time is reduced and the physical loss of sample through manipulation is avoided.

Experimental

Release and isolation of oligosaccharides

Eggs from *X. laevis* were collected and washed with De Boers buffer. The jelly coat layers were solubilized by mercaptoethanol and separated from the eggs. The jelly was dialyzed overnight in a MWC 10,000 kDa dialysis bag and subsequently lyophilized. O-linked oligosaccharides were released from egg jelly glycoproteins in 1.0 M $NaBH_4$ and 0.1 M NaOH. After incubating 19 hours at 48°C, Dowex (H^+ form) was added into the solution until it stopped bubbling. The solution was filtered and adjusted to pH 6.5 with 0.1 M NaOH and/or 0.1 M formic acid. The resulting mixture of oligosaccharides was distilled from methanol in a rotary evaporator up to six times to remove borates. A Bio-Gel P2 column (1.5×40 cm, Bio-Rad Laboratories, Hercules, CA) was used for desalting the oligosaccharide mixture. The eluent from the P2 column was collected in fractions and tested for the presence of oligosaccharides by the phenol-sulfuric acid assay using galactose as the standard. The same fractions were also tested by mass spectrometry. It was determined that mass spectrometry was more sensitive for detecting fractions that contained oligosaccharides. Fractions separated by the P2 column with detectable oligosaccharides were combined and further purified with a C18 cartridge.

Separation

The purified mixture from the combined neutral and anionic oligosaccharide P2 fractions was injected into the HPLC equipped with a primary amine column (4.6×250 mm, Supelco, Bellefonte, PA). A gradient of water and acetonitrile with a flow rate of 1.0 ml/min was used for the separation. The oligosaccharide alditols were detected at 206 nm. A total of 80 fractions were collected in one-minute intervals.

Mass spectrometry

MALDI-FTMS was performed on a commercial instrument (Ionspec, Irvine, CA) with a 4.7 T superconducting magnet [21]. The MALDI sample was prepared by concentrating 1 to 20 μL of the HPLC eluent directly on the probe. For the positive mode, 1.0 μL of 0.01 M NaCl or CsCl was added to the sample to give primarily sodiated or cesiated species, respectively. For the MALDI matrix, 2.0 μL of 0.4 M 2,5-dihydroxyacetophenone in ethanol was used. Hot air was used to crystallize quickly the sample on the probe. For the determination of neutral oligosaccharides in the negative mode, 1.0 μL of sulfuric acid (0.01 M) or sulfanilic acid (0.01 M) was used as anion dopants [22]. These acids coordinated with neutral oligosaccharides and provided the charge necessary for analysis in the negative mode. A nitrogen laser at 337 nm was used to ionize the samples.

For the singly charged anionic oligosaccharides, NH_4^+ resin was used on the probe tip to further remove any positively charged contaminant in the sample. The addition of the NH_4^+ resin significantly improved the signal of sulfated oligosaccharides. A 2.0 μL of saturated 2,5-dihydroxyacetophenone (DHAP) in ethanol was then added on the probe tip for the MALDI matrix. The MALDI crystals were formed under vacuum without removal of the resin and the sample was analyzed directly. For the analysis of doubly sulfated oligosaccharides, the NH_4^+ resin was first added to the sample solution in the vial. The sample was centrifuged and a small aliquot of the solution (1–5 μL) was then removed and placed on the probe tip. Matrix was added as before. The ambient concentration of sodium ions in the matrix and solution was sufficient to produce a singly charged species with one sodium coordinated to the doubly sulfated oligosaccharide.

Collision-induced dissociation

A desired ion is readily selected in the analyzer with the use of an arbitrary-wave form generator and a frequency synthesizer. All CID experiments were performed at +1000 Hz off resonance to the cyclotron frequency of the isolated ion. The CID excitation time was 1,000 milliseconds. Two pulses of argon were introduced into the analyzer chamber at 0 and 500 millisecond for collision gas. The excitation voltages ranged from 2.5 to 8.0 V depending on the desired level of fragmentation and the size of the oligosaccharide.

Results

Analyses of HPLC fractions

For this report, further HPLC separation of the pooled P2 eluent was performed. In Figure 1, the HPLC chromatogram is shown for a mixture of neutral and anionic O-linked oligosaccharides released from the egg jelly glycoproteins. The neutral components eluted in the first half of the chromatography run (peaks **C** to **L3**), while the anionic oligosaccharides eluted in the later fractions (**J1** to **P**). Peaks **A** and **B** were due to salts and other small molecular contaminants; no further analyses were performed on these fractions. We found it necessary to inspect each fraction with MALDI-FTMS as it generally had better sensitivity for oligosaccharides than the UV diode array detector of the HPLC.

The separation was generally incomplete with some HPLC fractions containing several oligosaccharides. For example, peak **C** contained at least three oligosaccharides (m/z 611, 716, and 757) while peak E contained four (m/z 821, 862, 919, 960). Isomers were sufficiently structurally unique that they eluted at different times. For example, m/z 757 is found at two different fractions (peak **C** and **D** in Figure 1). The CID spectra yielded two distinct fragmentation patterns due to two different oligosaccharides. Even when isomers eluted in the same peaks, they were often sufficiently resolved as the fraction containing the beginning of the peak will be richer in one component while the fraction containing the end of the peak is richer in another.

Tables 1, 2, and 3 summarize the HPLC fractions with the corresponding oligosaccharides. Two HPLC runs are provided for the neutral components (Table 1). An earlier run where the neutral and the anionic components were first separated in a charge exchange column was used for comparison (HPLC old) [21]. The compositions of the oligosaccharides are provided based on the exact masses. The neutral O-linked oligosaccharides from the whole egg jelly glycoproteins ranged in size from trisaccharides to octasaccharides. They were composed of fucoses (Fuc), hexoses (Hex), and *N*-acetylhexosamines (HexNAc). From the NMR study, the hexoses were most likely to be galactose [12]. The *N*-acetyl hexosamines were either *N*-acetylgalactosamine or *N*-acetylglucosamine.

The original pooled samples were from two different populations of *X. laevis*. The new HPLC run contained more neutral oligosaccharides as we became more experienced in detecting oligosaccharides. However, oligosaccharides were present in the previous sample that were not observed in this sample. The variations in oligosaccharides between populations and individuals are the subject of continuing studies in the group.

Determination of neutral oligosaccharide components

Differentiation of fragments from parent ions

Figure 2a shows the sodium-doped mass spectrum in the positive mode of the HPLC fraction collected at 33 minutes. There were many peaks in the spectrum that corresponded to oligosaccharides including m/z 449, 611, 773, 919, and 1065. One way to determine if any of these peaks are fragments is to decrease the laser fluence by purposely defocusing the laser. The result is shown in Figure 2b where only two peaks m/z 919 and 1065 are observed. This result indicated that the peaks at the lower mass range were indeed fragments. However the m/z 919 could still be a fragment of m/z 1065 via the loss of a fucose. When the same sample was doped with cesium chloride [23,24], one dominant peak remained corresponding to $[M + Cs]^+$ (Figure 2c). The m/z 133 in the spectrum corresponds to the bare cesium ion.

The same fraction was also doped with the H_2SO_4 (1.0 μL, 0.01 M) and analyzed in the negative mode. We previously

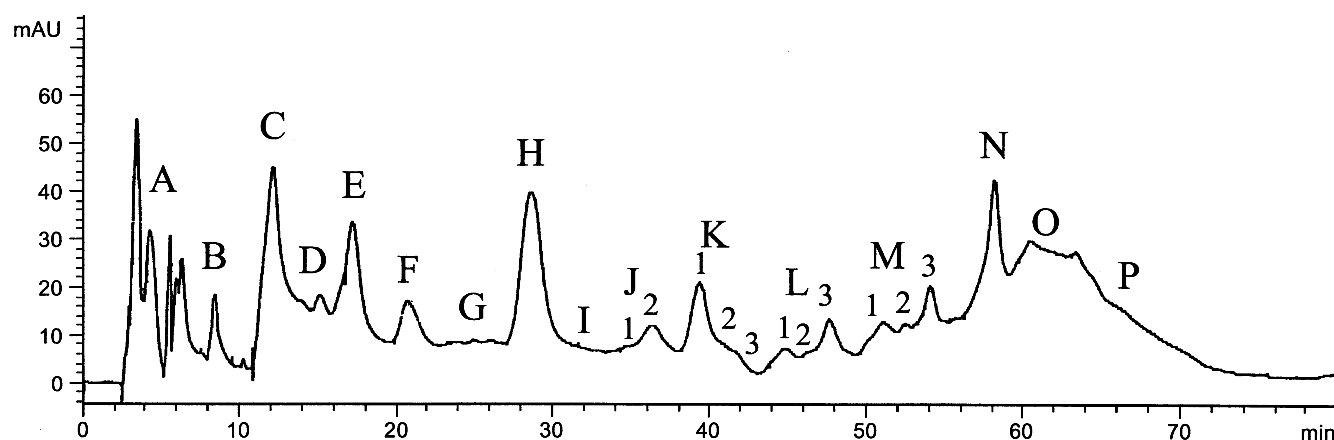

Figure 1. HPLC chromatogram of the O-linked oligosaccharide mixture released from egg jelly glycoproteins of *X. laevis*. A primary amine column was used with a flow rate of 1.0 mL water/acetonitrile gradient, and an UV detector set at the wavelength of 206 nm. Peaks C to L3 consisted of neutral components, and peaks J1 to P are anionic oligosaccharides. Peaks A and B do not have any detectable oligosaccharide.

Table 1. Neutral oligosaccharides

#	HPLC old	HPLC new	Theo. m/z	Expt. m/z	Hex:Fuc:HexNAc
1	C1	C	611.23	611.23	1:0:2
2	C1	C	757.28	757.28	1:1:2
3	C1	not found	659.24	/	2:2:0
4	C1	C	716.26	716.26	2:1:1
5	C2	D	757.29	757.28	1:1:2
6	D2	E	960.36	960.38	1:1:3
7	E	E	919.34	919.34	2:1:2
8	E	E	862.32	862.33	2:2:1
9	E	E	821.29	821.27	3:2:0
10	F	F	919.34	919.34	2:1:2
11	H	H	1065.40	1065.40	2:2:2
12	not shown	K1	1227.45	1227.45	3:2:2
13	D1	D	903.34	903.33	1:2:2
14	D2	D	903.34	903.33	1:2:2
15	F	F	1065.40	1065.40	2:2:2
16	G1	not found	919.34	/	2:1:2
17	G1	not found	1024.37	/	3:2:1
18	G1	not found	1389.50	/	4:2:2
19	G2	not found	1065.40	/	2:2:2
20	N/A	J2	1211.45	1211.44	2:3:2
21	N/A	J2	1227.45	1227.45	3:2:2
22	N/A	K1	1268.48	1268.46	2:2:3
23	N/A	K1	1268.48	1268.46	2:2:3
24	N/A	L1	1373.51	1373.53	3:3:2
25	N/A	L1	1389.50	1389.49	4:2:2
26	N/A	L3	1373.51	1373.53	3:3:2
27	N/A	L3	1389.50	1389.49	4:2:2
28	N/A	L3	1430.53	1430.48	3:2:3
29	N/A	L3	1430.53	1430.48	3:2:3

showed that HSO_4^- complexes to neutral oligosaccharides to produce quasimolecular ions without fragmentation [19]. Figure 2d shows a single quasimolecular with m/z 1139 corresponding to $[M + HSO_4]^-$. Sulfanilic acid used as dopant has been shown to produce stronger quasimolecular ions than HSO_4^- without fragments [22]. Figure 2e shows the quasimolecular ion to be m/z 1214, $[M + \text{sulfanilic acid-H}]^-$. Again, there are no peaks in the spectrum corresponding to fragment ions; sulfuric acid is present as contaminant in the sulfanilic acid solution producing the m/z 1139 peak. The m/z 1041 peak was the deprotonated neutral oligosaccharide. Peaks at the lower mass range corresponded to matrix and salt complexes.

Determination of neutral oligosaccharides from false neutral signals

The analysis of oligosaccharides in the positive mode with MALDI-FTMS sometimes produced false neutrals in addition to fragments. For example, anionic oligosaccharides when present in significant concentrations produced signals even in the positive mode. They yielded two ionic species in the positive mode corresponding to the metal-coordinated species and the neutral oligosaccharide product resulting from the loss of the sulfate group. Figure 3a shows a positive mode MALDI-FTMS spectrum with the base peak at the m/z 1265 that did not correspond to a sodium coordinated neutral oligosaccharide but rather a sulfated oligosaccharide with two sodium ions – one to neutralize and the other to provide the net positive charge. The m/z 1163 peak corresponded to the loss of the sulfate group and with the addition of a sodium cation. Figure 3b shows the mass spectrum of the same sample in the negative mode. The species with m/z 1219 was composed of 1 hexose, 1 fucose, 4 *N*-acetyl hexosamines, and one sulfate group, the same constituent as the m/z 1265 peak in the positive mode.

High-mass accuracy, another hallmark of FTMS is generally useful for rapidly identifying oligosaccharide components. For example, two peaks were observed in the MALDI/FTMS spectrum of fraction 52 that differed by a nominal 16 mass unit (Figure 4a). This difference could be due to an oxygen atom, which means the two species were distinct oligosaccharides, or the difference between a sodium and a potassium ion, a common interference in biological samples. The difference

Table 2. Singly sulfated oligosaccharide components

#	*Theo m/z*	*Hex*	*Fuc*	*HexNAc*	*sulfate*	*HPLC peaks*
1	975.298	2	1	2	1	K3,L1,L2,L3,M1
2	1016.324	1	1	3	1	K3
3	1201.355	5	2		1	K3
4	1219.404	1	1	4	1	K3,L1,L2,L3,M1
5	1363.408	6	2		1	L1,L2
6	1365.462	1	2	4	1	L1,L2 · · · M1
7	1178.377	2	1	3	1	L1,L3,M1
8	1349.467		3	4	1	L1 · · · L3
9	1073.346	1		4	1	L3
10	1381.456	2	1	4	1	M1,M2,M3
11	1511.520	1	3	4	1	M2,M3
12	1584.536	2	1	5	1	M2,M3
13	1527.514	2	2	4	1	M3
14	829.240	2		2	1	N
15	1486.488	3	2	3	1	N
16	1657.577	1	4	4	1	N
17	1673.572	2	3	4	1	N
18	1933.673	2	2	6	1	N
19	975.298	2	1	2	1	N
20	1178.377	2	1	3	1	N
21	1673.572	2	3	4	1	N
22	1787.615	2	1	6	1	N
23	1137.350	3	1	2	1	N
24	1219.404	1	1	4	1	N,O
25	1235.399	2		4	1	N,O
26	1381.456	2	1	4	1	N,O,P
27	1324.435	2	2	3	1	O
28	1527.514	2	2	4	1	O,P
29	1997.678	4	3	4	1	O
30	2225.789	2	4	6	1	O,P
31	2298.805	3	2	7	1	O,P
32	1235.399	2		4	1	P
33	1324.435	2	2	3	1	P
34	1340.430	3	1	3	1	P
35	1673.572	2	3	4	1	P
36	1892.647	3	2	5	1	P
37	829.240	2		2	1	P
38	2444.864	3	3	7	1	P
39	2362.810	5	3	5	1	P
40	2403.837	4	3	6	1	P
41	2590.921	3	4	7	1	P

Table 3. Doubly sulfated oligosaccharide components

#	*Theo m/z*	*Hex*	*Fuc*	*HexNAc*	*sulfate*	*Na^+*	*fractions*
1	931.179	2		2	2	1	N
2	1077.236	2	1	2	2	1	N
3	1280.316	2	1	3	2	1	N
4	1483.395	2	1	4	2	1	N,O,P
5	1629.453	2	2	4	2	1	P
6	1588.427	3	2	3	2	1	P

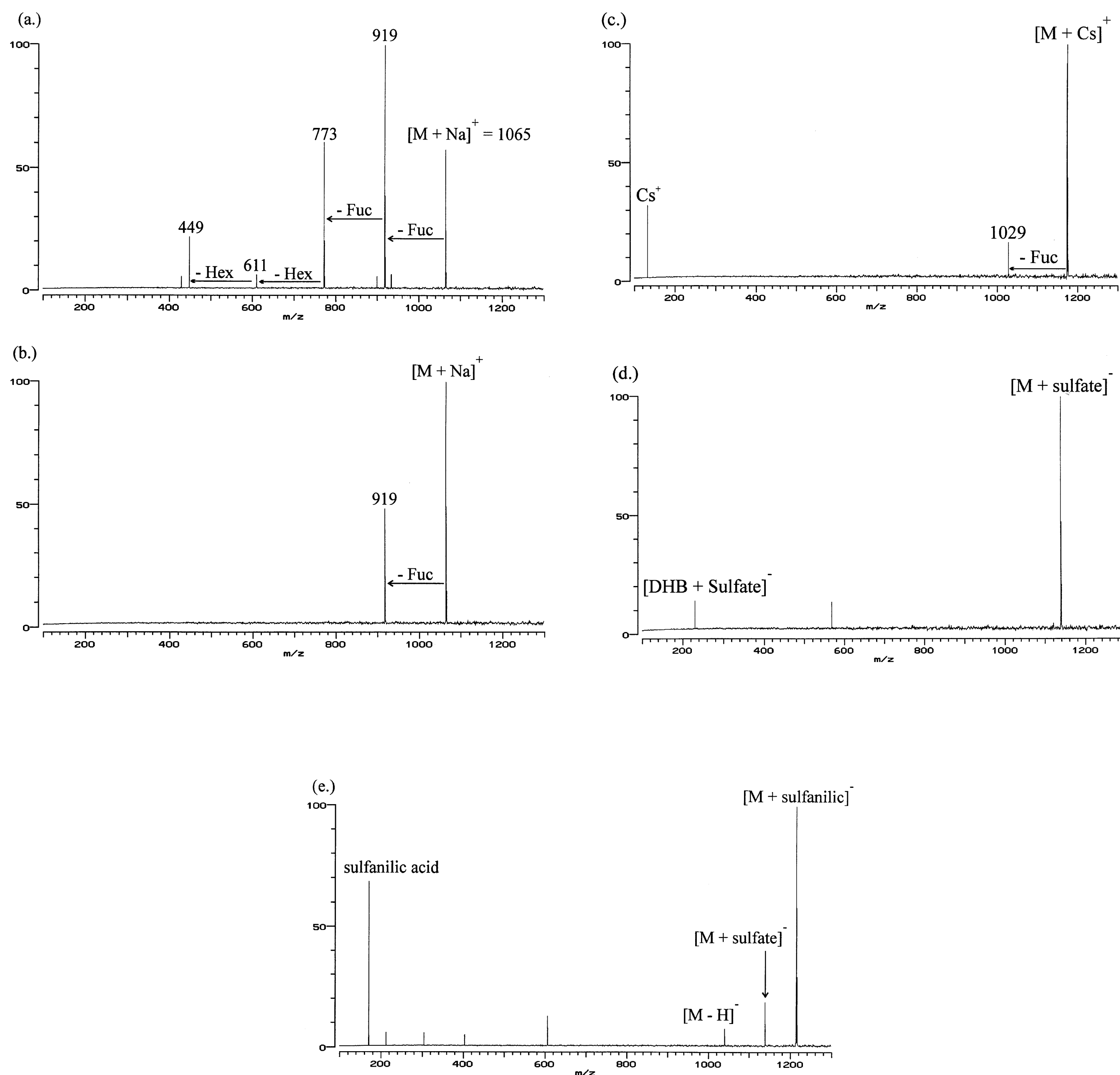

Figure 2. MALDI-FTMS spectra of the amine HPLC fraction collected at 33 minutes in the positive mode. (a) Under the normal experimental condition using sodium ions as the dopant, the extensive fragmentation made the assignment of molecular ions difficult. The amount of fragmentation can be reduced by (b) purposely unfocusing the laser or use larger alkali metal, *e.g.*, (c) cesium ions as the dopant. Using anionic dopant, (d) sulfate and (e) sulfanilic acid, any fragmentation was completely eliminated, making the assignment of molecular ions straightforward in the negative mode.

between the two signals (*m/z* 1389.5276 and *m/z* 1373.5926) is 15.998 mass units, which is closer to the mass of an oxygen atom (15.995 mu) than the difference between a potassium and a sodium ion (15.974). For confirmation, the sample was doped with cesium chloride producing a spectrum with two major peaks corresponding to shifts of 110 mass units relative to the sodium chloride doped sample (Figure 4b) – the mass difference between Na^+ and Cs^+.

The most definitive method for assessing suspect signals is by performing CID at sufficiently high translational energy to yield compositional information. Based on the exact mass, the *m/z* 1374 peak was computed to contain 3 Hex, 3 Fuc, and 2 HexNAc, and the *m/z* 1390 peak consisted of 4 Hex, 2 Fuc, and 2 HexNAc. From CID fragments of the isolated molecular ions, these two peaks were determined to be different oligosaccharides with the predicted compositions. Figure 5a

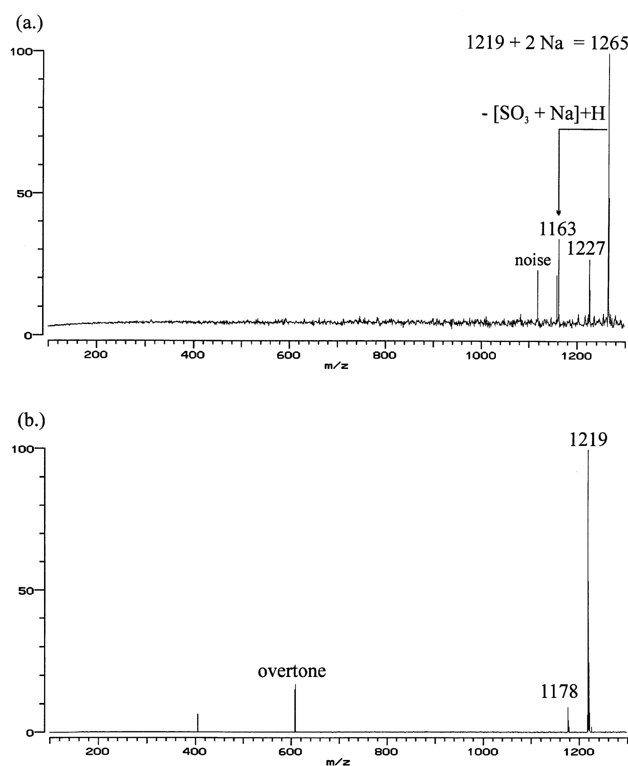

Figure 3. (a) A false signal resulting from a strong sulfated oligosaccharide coordinated to two sodium ions in the positive mode, and (b) the same sulfated oligosaccharide in the negative mode.

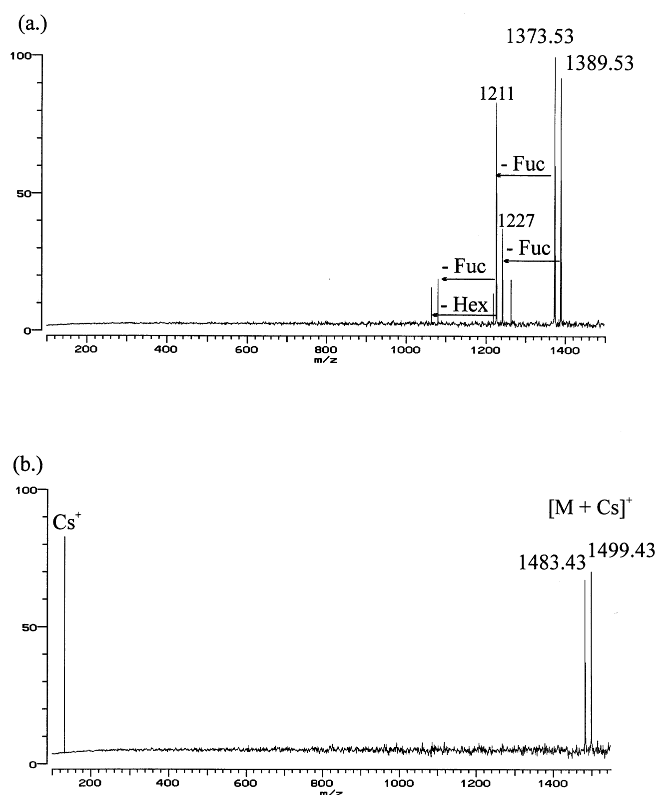

Figure 4. MALDI-FTMS spectra of the amine HPLC fraction collected at 52 minutes: (a) doped with sodium ions and (b) doped with cesium ions.

and 5b show the CID spectra of the *m/z* 1374 peak with the base-to-peak excitation voltages at 6 V and 8 V respectively. Figure 6a and 6b show the CID spectra of the *m/z* 1389 peak with the base-to-peak excitation voltages at 5 V and 9 V respectively.

Structural determination of neutral components

We have recently illustrated that the complete structural elucidation of unknown components can be determined with primarily mass spectrometry [25]. In an oligosaccharide mixture (or library) released from the same biological source, the components are usually composed of a finite number of substructural motifs that combine to give rise to heterogeneity. The key is to identify the motifs and their corresponding CID pattern. The structures of unknown components are then obtained solely from the CID spectra. Multiple stages of MS are necessary (MS^2 and as much as MS^4) to produce the fragmentation pattern unique for each motif.

The motifs for *X. laevis* have been published in the earlier report (Chart 1). They were obtained from the systematic CID studies of oligosaccharides that were initially elucidated by Strecker and coworkers using NMR [12]. Each motif in Chart 1 yielded a distinct and identifiable fragmentation pattern that was conserved from one compound to another [25]. Variations in the linkage and the configuration at the anomeric carbon are sometimes differentiated. For example, motif **ii** and **iii** vary by one linkage, but the two motifs yield noticeably different CID patterns [25]. Moreover, we have confirmed the structures proposed by this method by using glycosidase digestion and mass spectrometry [26]. It should be emphasized that without the motif information, CID alone provides only the rudimentary information regarding connectivity as the alditols do not yield the cross-ring cleavages necessary for obtaining linkage information. This motif-based analysis, which we term the catalog-library approach (CLA) because a catalog of motif is developed to determine the structures in the library, was used to determine the structure of a few of the neutral oligosaccharide components in the earlier publication. It is used in this report to determine all the neutral oligosaccharide components of the jelly coat of *X. laevis*.

An example of how the catalog was used to elucidate structures in the library is illustrated with a component having *m/z* 1373 obtained from fraction 52 (L1 in the HPLC). The composition of the oligosaccharide was predicted from the exact mass to be 3 Hex, 3 Fuc, and 2 HexNAc (Table 1). With the CID excitation voltage of 6.0 V, the *m/z* 1373 peak fragmented extensively down to one monosaccharide unit (Figure 5a). Motif **ii** was present as characterized by the loss of

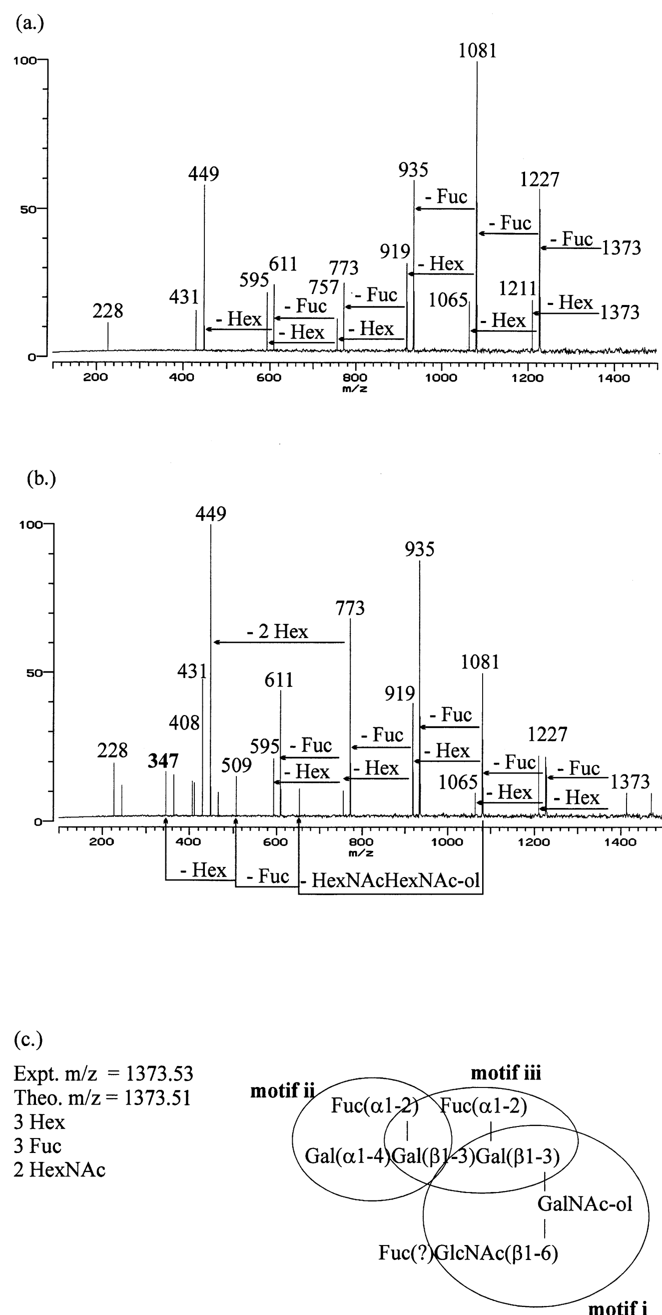

Figure 5. CID spectra of m/z 1374 peak in fraction 52 with the base-to-peak excitation voltages of (a) 6 V and (b) 8 V. (c) The CID spectra were interpreted using CLA to obtained sub-structures that were linked to provide the whole structure of the oligosaccharide.

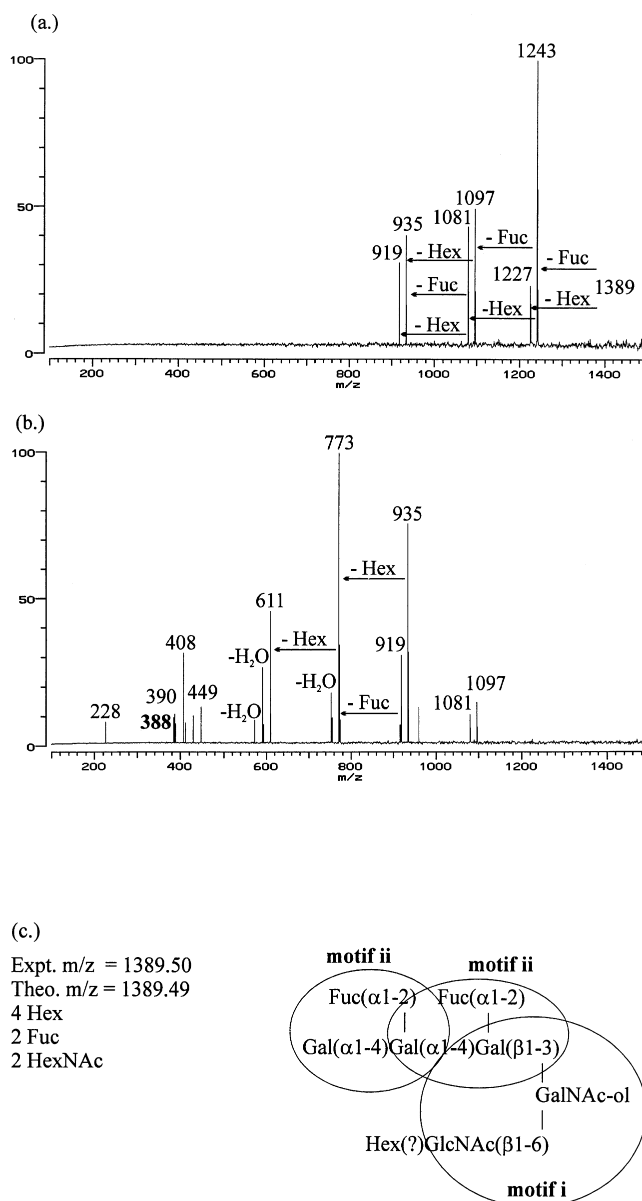

Figure 6. CID spectra of m/z 1389 peak in the fraction 52 with the base-to-peak excitation voltages of (a) 5 V and (b) 9 V. Using CLA, the proposed structure is shown in (c).

a Hex unit (162u) and a Fuc unit (146u) from the quasimolecular ion (Chart 1). Note the nearly equal abundances of m/z 1227 and 1211 particularly in Figure 5b. For motif **ii** the loss of 162 u is always strong (> 30%) relative to the loss of 146. Motif **iii**, the isomer of motif **ii**, rarely produces loss of 162 u from the quasimolecular ion. When present the fragment is always less than 10% relative to the loss of 146u regardless of the excitation energy. However, in this compound motif **iii** was also present as characterized by the presence of m/z 347. This fragment corresponded to a Gal(β1-3)Gal(β1-3) unit coordinated to Na^+. In general, this unit does not readily fragment along the glycosidic bond, unlike the Gal(α1-4)Gal unit. The loss of two hex units Gal(β1-3)Gal(β1-3) from m/z 773 to yield a strong m/z 449 signal is consistent with this finding. Also present in the spectra was motif **i** as evidenced by the peaks m/z 611, 449, 408, 431, and 413. Based on the three motifs the proposed structure is given in Figure 5c.

A second neutral component was present in L1 with the quasimolecular ion m/z 1389.50 corresponding to 4 Hex,

	Structure	Characteristic Signals
i.	Gal(β1-3) | GalNAc-ol | GlcNAc(β1-6)	*m/z* 611, 449, 408 also m/z 431, 413
ii.	Fuc(α1-2) | Gal(α1-4)Gal-	Loss of Gal (162u) and Fuc(146u) from [M+Na]$^+$. Loss of Gal 30-100% relative to loss of Fuc.
iii.	Fuc(α1-2) | Gal(β1-3)Gal(β1-3)-	*m/z* 347 + Loss of Gal (162u) and Fuc(146u) from [M+Na]$^+$. Loss of Gal less than 10% minor (less than relative to loss of Fuc)
iv.	Non-branched reducing end - Gal(β1-3)GalNAc-ol | Fuc(α1-2)	Loss of reducing end, GalNAc-ol (-223u)
v.	Branched reducing end - GalNAc(α1-3) | Fuc(α1-2)- Gal-ol **or** - Gal(β1-3) | Fuc(α1-2)- Gal-ol	m/z 205, loss of m/z 182

Chart 1. Catalog of substructure motifs.

2 Fuc, and 2 HexNAc. The MS/MS spectra produced under two CID conditions, 5.0 and 9.0 V, are shown in Figure 6. The strong m/z 1227 (loss of 162u) indicates the presence of motif **ii** (Figure 6a). Increasing the collision energy with 7.0 V increased the relative intensity of m/z 1227 further (Spectrum not shown). The strong relative abundances of the peaks corresponding to losses of Hex and Fuc in m/z 1097, 1081, respectively, and m/z 935, 919 suggested the presence of a second Gal(α1-4)Gal group (Figure 6b). The presence of m/z 611, 449, 408, 431, and 413 again gave rise to motif **i**. There was an additional Hex whose identity and connectivity was unknown. However, the presence of m/z 388 in the CID spectrum indicated a Hex-GlcNAc combination. The proposed structure is presented in Figure 6c.

The complete list of all neutral oligosaccharides found in the jelly coat of *Xenopus laevis* are presented in Chart 2. From a total of 29 neutrals detected, the structures of 24 were identified or elucidated. In this report, five new oligosaccharides were elucidated.

Determination of anionic oligosaccharides components

The structural elucidation of the anionic components proved to be significantly more difficult than the neutral components. In general, we obtained less material for the anionic than the neutral. We suspect this to be due to the harshness of the release method, which may remove the sulfate ester, rather than some biological factor. There have been a few reported structures of sulfated and sialylated oligosaccharides from *X. laevis* by Strecker [12,27], but they are not of sufficient number to produce a catalog of substructural motifs. This limitation made it difficult to obtain complete structures from CID alone. Nonetheless, CID still provided critical structural information such as relative connectivity of the hexose, fucose, and *N*-acetylhexose residues, and the relative positions of the sulfate group.

A total of 41 O-linked singly sulfated (Table 2) and six doubly sulfated (Table 3) oligosaccharide components were detected by MALDI-FTMS. Sialylated oligosaccharides were also observed but these species were suppressed both in the positive and negative mode in MALDI-FTMS [28]. All anionic oligosaccharides were observed as -1 charged state in the negative mode MALDI-FTMS. Only the theoretical m/z is listed in the tables as this varied from the observed m/z by less than 0.01 mass units. These oligosaccharides ranged in size from 4 to 14 residues and their composition (hexose, fucose, *N*-acetylhexosamine) were assigned based on the exact mass. For singly sulfated oligosaccharides, the corresponding $[M-H]^-$ peaks were observed. Doubly sulfated oligosaccharides, on the other hand, combined with one sodium ion to form the quasimolecular ion $[M-2H+Na]^-$. No doubly charged peaks under the MALDI-FTMS condition were observed. MALDI-FTMS was also performed in the positive mode but this produced much weaker signals while no additional structural information was obtained.

CID was performed on the most abundant constituents. An example of the structural information obtained from CID is illustrated with an anionic oligosaccharide component also present in the peak K3 (Figure 1). This singly sulfated oligosaccharide with m/z 1016 is composed of 1-Hex, 1-Fuc, and 3-HexNAc units (Table 2). Off-resonance CID (4 V, peak-peak, Figure 7b) yielded the fragment m/z 282 consistent with a $[HexNAc\text{-}SO_3]^-$ group. The absence of the loss of a HexNAc-ol group from the quasimolecular ion (m/z 1016) suggested that the oligosaccharide was branched at the non-reducing end. One branch was a single residue corresponding to $[HexNAc\text{-}SO_3]^-$, which was deduced from the presence of a m/z 505 fragment [SO_3-HexNAc-HexNAc-ol]. The other branch was composed of a Hex and a HexNAc unit, consistent with the loss of 365 mass units from m/z 870 to yield m/z 505. Based on the MS/MS spectrum, it was unclear whether Hex or HexNAC was directly linked to the reducing-end HexNAc-ol group. An additional stage of MS was performed on the m/z 870 fragment. The resulting MS/MS/MS spectrum (Figure 7b) yielded the presence of m/z 667 indicating that the Hex residue was directly linked to the reducing-end. The proposed structure is presented in Chart 3 (m/z 1016).

Sulfate ester formation adds another level of complexity that significantly increases the number of isomers and the overall heterogeneity of the sample. For example, two components with identical m/z 829 were observed in Peak N and Peak P of the HPLC trace. The singly sulfated oligosaccharide was composed

1
GlcNAc(β1-6)
GalNAc-ol
Gal(β1-3)

5
GlcNAc(β1-6)
GalNAc-ol
Fuc(α1-2)Gal(β1-3)

7
GlcNAc(β1-6)
GalNAc-ol
Gal(α1-4)Gal(β1-3)
Fuc(α1-2)

10
GlcNAc(β1-6)
GalNAc-ol
Gal(β1-3)Gal(β1-3)
Fuc(α1-2)

11
GlcNAc(β1-6)
GalNAc-ol
Fuc(α1-2)Gal(β1-3)Gal(β1-3)
Fuc(α1-2)

12
GlcNAc(β1-6)
GalNAc-ol
Gal(α1-4)Gal(β1-3)Gal(β1-3)
Fuc(α1-2) Fuc(α1-2)

14
Fuc ~ [GlcNAc(β1-6) / GalNAc-ol / Fuc(α1-2)Gal(β1-3)]

15
GlcNAc(β1-6)
GalNAc-ol
Fuc(α1-2)Gal(α1-4)Gal(β1-3)
Fuc(α1-2)

16
Fuc ~ [Gal(?)GlcNAc(β1-6) / GalNAc-ol / Gal(β1-3)]

19
Fuc(α1-2)Gal(?)GlcNAc(β1-6)
GalNAc-ol
Fuc(α1-2)Gal(β1-3)

20
Fuc(?)GlcNAc(β1-6)
GalNAc-ol
Fuc(α1-2)Gal(β1-3)Gal(β1-3)
Fuc(α1-2)

21
GlcNAc(β1-6)
GalNAc-ol
Fuc(α1-2)Gal(α1-4)Gal(α1-4)Gal(β1-3)
Fuc(α1-2)

22
GlcNAc(β1-6)
GalNAc-ol
HexNAc(?)Gal(β1-3)Gal(β1-3)
Fuc(α1-2) Fuc(α1-2)

24
Fuc(?)GlcNAc(β1-6)
GalNAc-ol
Gal(α1-4)Gal(β1-3)Gal(β1-3)
Fuc(α1-2) Fuc(α1-2)

25
Hex(?)GlcNAc(β1-6)
GalNAc-ol
Gal(α1-4)Gal(α1-4)Gal(β1-3)
Fuc(α1-2) Fuc(α1-2)

26
GlcNAc(β1-6)
GalNAc-ol
Fuc(α1-2)Gal(β1-3)Gal(β1-3)Gal(β1-3)
Fuc(α1-2) Fuc(α1-2)

4
Gal(α1-4)Gal(β1-3)GalNAc-ol
Fuc(α1-2)

6
GlcNAc(α1-3)GalNAc(α1-3)Gal(β1-3)GalNAc-ol
Fuc(α1-2)

8
Fuc(α1-2)Gal(β1-3)Gal(β1-3)GalNAc-ol
Fuc(α1-2)

17
Gal(α1-4)Gal(β1-3)Gal(β1-3)GalNAc-ol
Fuc(α1-2) Fuc(α1-2)

2
Fuc(α1-2)
Gal-ol
GlcNAc(α1-3)GalNAc(β1-3)

9
Fuc(α1-2)
Gal-ol
Gal(α1-4)Gal(β1-3)
Fuc(α1-2)

3
Fuc(α1-2)
Gal-ol
Fuc(α1-2)Gal(β1-3)

13
Fuc ~ [Fuc(α1-2) / Gal-ol / GlcNAc(α1-3)GalNAc(α1-3)]

Chart 2. Neutral oligosaccharides from egg jelly coats of *X. Laevis.*

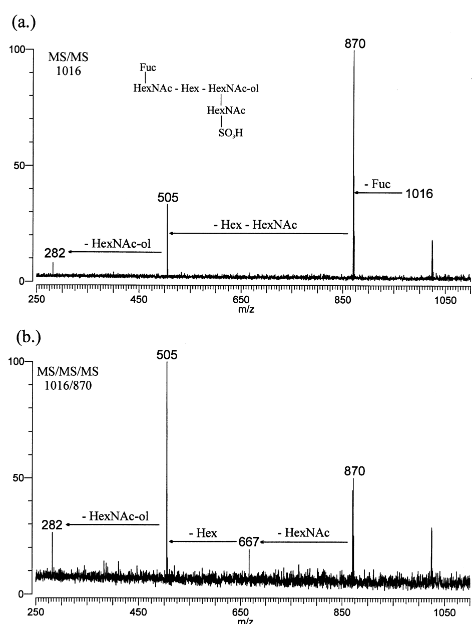

Figure 7. CID spectra of anionic component m/z 1016 in the negative mode. (a) MS/MS spectrum and (b) MS/MS/MS spectrum (m/z 1016 -> m/z 870 ->). The presence of m/z 667 yields a Hex connected to the reducing end group.

of two Hex and two HexNAc. CID was performed on the ion obtained by sampling the center of HPLC peak N to yield the spectrum in Figure 8a. The loss of a Hex followed by a HexNAc-ol and a HexNAc indicated a sequential fragmentation starting with one terminus (Hex), through the branched reducing end (HexNAc-ol), to the other antenna HexNAc and the Hex-SO_3^- terminus that retained the charge. The fragmentation pattern was consistent with a single compound whose structure is shown (inset). The CID spectrum of m/z 829 from the tail end of HPLC Peak N produced an additional fragment, m/z 505 (Figure 8b). This fragment ion corresponded to the loss of two Hex. However because m/z 241 is a $[Hex + SO_3]^-$ peak, the m/z 505 fragment must be due to a second, less abundant component with a $[HexNAc + SO_3]^-$ residue that is not observed in the mass spectrum. The lack of additional fragments made it impossible to further elucidate this structure.

The partial structures of 13 were determined from the total of 47 singly and doubly sulfated oligosaccharides. The smaller group was sufficiently isolated in pure form to obtain unambiguous spectra such as that presented in Figure 7 and 8a. In a recent publication, Strecker and co-workers presented the structure of six sulfated oligosaccharides determined by NMR [27]. There were only two compounds that were found

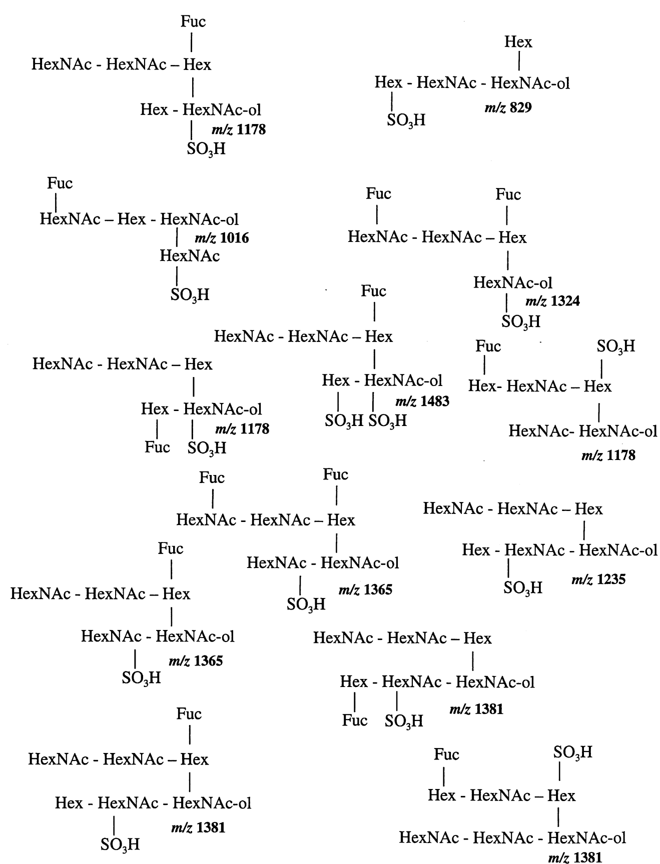

Chart 3.

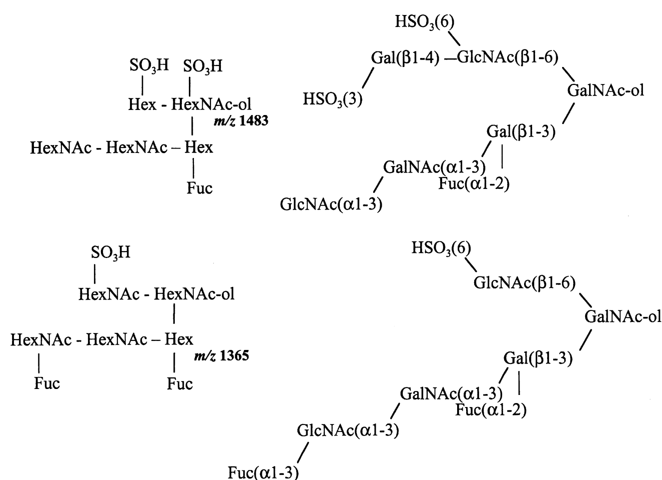

Scheme 1.

in both the NMR and the MS analyses. The structures of these compounds matched exactly (Scheme 1). Nonetheless, this represents a significantly lesser degree of correspondence than that obtained for the neutral species where essentially all neutral species that were elucidated by NMR have been elucidated by mass spectrometry. It also points to the general difficulty in elucidating structures of sulfated oligosaccharides.

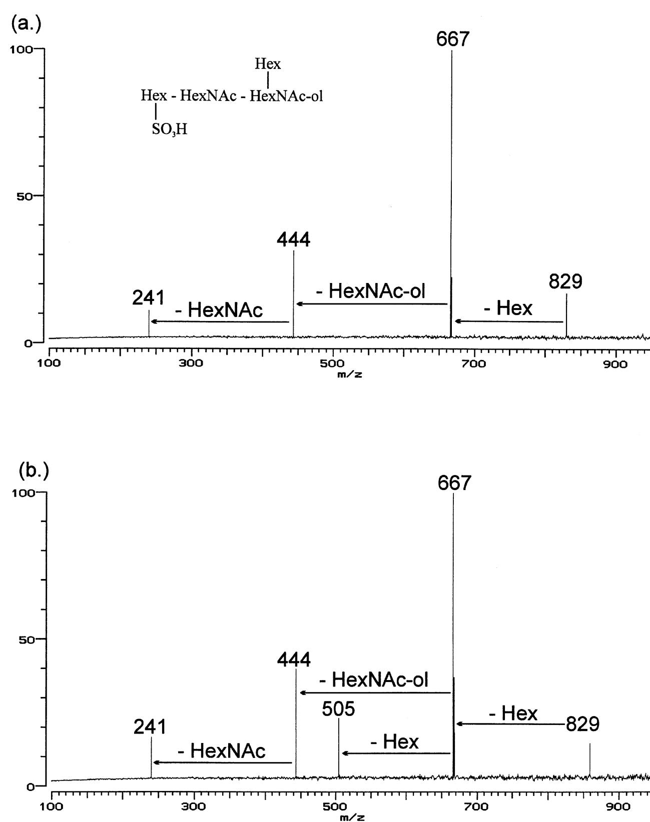

Figure 8. CID spectra of anionic component m/z 829 in the negative mode. (a) MS/MS spectrum of m/z 829 from the center of peak N in the HPLC chromatogram. (b) MS/MS of m/z 829 in the last part of peak N. The spectrum yields the presence of an isomer with m/z 505.

Conclusion

A strategic method is described to profile oligosaccharide libraries from a specific biological source. The procedure for the analysis of a complex mixture is simplified. The FTMS analysis effectively reduced a substantial amount of purification work traditionally done by chromatography and electrophoresis. The isolation of individual components is achieved with some rudimentary HPLC separation, but final separation was performed in the mass analyzer of the mass spectrometer. The specific separation of neutral and acidic components was unnecessary as the FTMS has the ability to analyze easily in both positive and negative modes. Furthermore, chemical interferences were minimal at low masses and were readily discerned from the real signal.

Although at the present, this method is specific for the egg jelly coat of *Xenopus laevis*, a similar method may be developed for any oligosaccharide library. A new biological source may, however, require a new catalog based on a different group of substructural motifs. The motifs may be established

by NMR or with the use of glycosidases in conjunction with mass spectrometry. However, once the catalog is developed then the structural elucidation of all other components, even those with concentrations that are too low as to preclude NMR analysis, may be determined. At this point, then biological problems may be asked. Each oligosaccharide has a distinctive fragmentation pattern which can be readily identified. In the future, better separation could mean retention time and molecular masses would be sufficient for complete identification.

Acknowledgment

Funding provided by the National Institutes of Health is gratefully acknowledged. The authors also wish to thank the reviewers for their many helpful comments.

References

1 Varki A, Biological roles of oligosaccharides: all the theories are correct, *Glycobiology* **3**, 97–130 (1993).
2 Hedrick JL, Nishihara T, Structure and function of the extracellular matrix of anuran eggs, *J Electron Microsc Tech* **17**, 319–35 (1991).
3 Hedrick JL, Hardy DM, In *Methods in Cell Biology*, Vol. 36. (Academic Press, NY, 1991), pp. 231–47.
4 Mozingo NM, Hedrick JL, Distribution of lectin binding sites in Xenopus laevis egg jelly, *Developmental Bio* **210**, 428–39 (1999).
5 Larabell C, Chandler DE, Fertilization changes in the vitelline envelope of echinoderm and amphibian eggs – self-assembly of an extracellular matrix, *J Electron Microsc Tech* **17**, 294–318 (1991).
6 Katagiri C, Role of oviducal secretions in mediating gamete fusion in anuran amphibians, *Zool Sci* **4**, 1–14 (1987).
7 Koyota S, Wimalasir SKM, Hoshi M, Structure of the main saccharide chain in the acrosome reaction-inducing substance of the startish, Asterial amurensis, *J Biol Chem* **272**, 10372–6 (1997).
8 Alves AP, Mulloy B, Diniz JA, Mourao PAS, Sulfated polysaccharides from the egg jelly layer are species-specific inducers of acrosomal reactions in sperms of sea urchins, *J Biol Chem* **272**, 6965–71 (1997).
9 Hedrick JL, Vo LH, The glycobiology of the acrsome reaction, *J Reprod Devel* **44** (suppl.), 15 (1998).
10 Bonnell BS, Smith SG, Hedrick JL, Microscopy of Glycoproteins, *Anal Biochem* **271**, 91–3 (1999).
11 Plancke Y, Wieruszeski JM, Alonso C, Boilly B, Strecker G, Structure of four acidic oligosaccharides from the jelly coat surrounding the eggs of Xenopus Laevis, *Eur J Biochem* **231**, 434–9 (1995).
12 Strecker G, Wieruszeski J-M, Plancke Y, Boilly B, Primary structure of 12 neutral oligosaccharide-alditols released from the jelly coats of the anuran Xenopus laevis by reductive beta-elimination, *Glycobiology* **5**, 137–46 (1995).
13 Yang Y, Orlando R, Simplifying the Exoglycosidase Digestion/MALDI-MS Procedures for Sequencing N-Linked Carbohydrate Side Chains, *Anal Chem* **68**, 570–2 (1996).
14 Küster B, Naven TJP, Harvey DJ, Rapid approach for sequencing neutral oligosaccharides by exoglysidase digestion and matrix-assisted laser desorption/ionization time-of-flight mass spectrometry, *J Mass Spectrom* **31**, 1131–40 (1996).
15 Dell A, FAB-mass spectrometry of carbohydrates, *Adv Carbohydr Chem Biochem* **45**, 19–72 (1987).
16 Domon B, Costello CE, A systematic nomenclature for carbohydrate fragmentations in FAB-MS/MS spectra of glycoconjugates, *Glycoconjugate J* **5**, 397–409 (1988).
17 Harvey DJ, Quantitative aspects of the matrix-assisted laser desorption ionization mass spectrometry of complex oligosaccharides, *Rapid Commun Mass Spectrom* **7**, 614–9 (1993).
18 Hofmeister GE, Zhou Z, Leary JA, Linkage position determination in lithium-cationized disaccharides: Tandem mass spectrometry and semiempirical calculations, *J Am Chem Soc* **113**, 5964–70 (1991).
19 Wong AWC, Voss MT, Lebrilla LR, An anion dopant for oligosaccharides in matrix-assisted laser desorption/ionization mass spectrometry, *Anal Chem* **71**, 205–11 (1999).
20 Cancilla MT, Penn SG, Lebrilla CB, Alkaline degradation of oligosaccharides coupled with matrix-assisted laser desorption/ionization – Fourier transform mass spectrometry, a new method for sequencing oligosaccharides, *Anal Chem* **70**, 663–72 (1998).
21 Tseng K, Lindsay LL, Penn SG, Hedrick JL, Lebrilla CB, Characterization of neutral oligosaccharide-alditols from Xenopus laevis jelly coats by matrix assisted laser Desorption Fourier transform mass spectrometry, *Anal Biochem* **250**, 18–28 (1997).
22 Wong AW, Wang H, Lebrilla CB, Selection of anionic dopant for quantifying desialylation reactions with MALDI-FTMS, *Anal Chem* **72**, 1419–25 (2000).
23 Cancilla MT, Wong AW, Voss LR, Lebrilla CB, Fragmentation reactions in the mass spectrometry of neutral oligosaccharides, *Anal Chem* **71**, 3206–18 (1999).
24 Cancilla MT, Penn SG, Carroll JA, Lebrilla CB, Coordination of alkali metals to oligosaccharide dictates fragmentation behavior in matrix-assited laser desorption/ionization Fourier transform mass spectrometry, *J Am Chem Soc* **118**, 6736–45 (1996).
25 Tseng K, Hedrick JL, Lebrilla CB, The catalog-library approach for the rapid and sensitive structural elucidation of oligosaccharides, *Anal Chem* **71**, 3747–54 (1999).
26 Xie Y, Tseng K, Hedrick JL, Lebrilla CB, Structural refinement and confirmation of neutral o-lined oligosaccharides by coupling exoglycosidase digestion and MALDI-FTMS, *J Am Soc Mass Spectrom* **12**, 877–84 (2001).
27 Guerardel Y, Kol O, Maes E, Lefebvre T, Boilly B, Davril M, Strecker G, O-Glycan variability of egg-jelly mucins from Xenopus laevis: Characterization of four phenotypes that differ by the terminal glycosylation of their mucins, *Biochem J* **352**, 449–63 (2001).
28 An HJ, Lebrilla CB, Suppression of sialylated by sulfated oligosaccharides in negative MALDI-FTMS, *Israel J Chem*, in press (2001).

Received 22 May 2001; revised 20 August 2001; accepted 23 August 2001